Earth and Planetary Science Letters 487 (2018) 74–83

Contents lists available at ScienceDirect

Earth and Planetary Science Letters

www.elsevier.com/locate/epsl

Magnesium isotopic evidence for chemical disequilibrium among cumulus minerals in layered mafic intrusion

Lie-Meng Chen [a,*], Fang-Zhen Teng [b,*], Xie-Yan Song [a], Rui-Zhong Hu [a], Song-Yue Yu [a], Dan Zhu [a], Jian Kang [a,c]

[a] State Key Laboratory of Ore Deposit Geochemistry, Institute of Geochemistry, Chinese Academy of Sciences, Guiyang 550081, PR China
[b] Isotope Laboratory, Department of Earth and Space Sciences, University of Washington, Seattle, WA 98195, USA
[c] University of Chinese Academy of Sciences, Beijing 100049, PR China

ARTICLE INFO

Article history:
Received 6 December 2017
Received in revised form 25 January 2018
Accepted 31 January 2018
Available online 9 February 2018
Editor: F. Moynier

Keywords:
magnesium isotopes
kinetic isotope fractionation
chemical diffusion
compositional zoning
Baima mafic intrusion

ABSTRACT

Magnesium isotopic compositions of olivine, clinopyroxene, and ilmenite from the Baima intrusion, SW China, for the first time, are investigated to constrain the magnitude and mechanisms of Mg isotope fractionation among cumulus minerals in layered mafic intrusions and to evaluate their geological implications. Olivine and clinopyroxene have limited Mg isotope variations, with δ^{26}Mg ranging from −0.33 to +0.05‰ and from −0.29 to −0.13‰, respectively, similar to those of mantle xenolithic peridotites. By contrast, ilmenites display extremely large Mg isotopic variation, with δ^{26}Mg ranging from −0.50 to +1.90‰. The large inter-mineral fractionations of Mg isotopes between ilmenite and silicates may reflect both equilibrium and kinetic processes. A few ilmenites have lighter Mg isotopic compositions than coexisting silicates and contain high MgO contents without compositional zoning, indicating equilibrium fractionation. The implication is that the light Mg isotopic compositions of lunar high-Ti basalts may result from an isotopically light source enriched in cumulate ilmenites. On the other hand, most ilmenites have heavy Mg isotopic compositions, coupled with high MgO concentration and chemical zoning, which can be quantitatively modeled by kinetic Mg isotope fractionations induced by subsolidus Mg–Fe exchange between ilmenite and ferromagnesian silicates during the cooling of the Baima intrusion. The extensive occurrence of kinetic Mg isotope fractionation in ilmenites implies the possibility of widespread compositional disequilibrium among igneous minerals in magma chambers. Consequently, disequilibrium effects need to be considered in studies of basaltic magma evolution, magma chamber processes, and magmatic Fe–Ti oxide ore genesis.

1. Introduction

Investigation of layered mafic intrusions can help to understand basaltic magma emplacement and differentiation, crystal accumulation, and magmatic base and precious metal mineralization (e.g., Cr, V, Ti, Fe, and platinum group elements) in crustal magma chambers (Namur et al., 2015; Scoates and Wall, 2015). Based on two long-standing views: (1) elements diffuse very fast during magmatic processes and (2) magma chambers cool slowly during formation of mafic intrusions, it is generally assumed that cumulus minerals in magma chambers are in thermodynamic equilibrium with each other. Such an assumption is a prerequisite for using cumulus mineral compositions to evaluate magmatic evolution and petrogenesis of cumulate rocks as were often done. However, recent studies have found that extensive disequilibrium isotope fractionation caused by chemical diffusion widely occurs in igneous minerals and rocks (e.g., Teng et al., 2011; Chopra et al., 2012; Sio et al., 2013; Oeser et al., 2015; Pogge von Strandmann et al., 2015; Richter et al., 2016; Xiao et al., 2016; Collinet et al., 2017). For example, olivine phenocrysts from the Kilauea Iki lava lake (Hawaii) display large kinetic Mg and Fe isotope fractionations, indicative of Mg–Fe inter-diffusion between olivine and evolved melts during magma differentiation (Teng et al., 2011; Sio et al., 2013). Whether or not kinetic processes can occur among cumulus minerals in mafic magma chambers remains uncertain.

Studies of Mg isotopic compositions of cumulus minerals (olivine, clinopyroxene, and ilmenite) in layered mafic intrusions could provide key insights into whether cumulus minerals are in equilibrium or not. In this study, we find for the first time that ilmenites display extremely large Mg isotopic variation (up to 2.4‰ in ^{26}Mg/^{24}Mg) and most times are heavier than coexisting olivine

* Corresponding authors.
E-mail addresses: chenliemeng@vip.gyig.ac.cn (L.-M. Chen), fteng@u.washington.edu (F.-Z. Teng).

https://doi.org/10.1016/j.epsl.2018.01.036
0012-821X/

and clinopyroxene in the Baima layered mafic intrusion, located at the central part of the Emeishan large igneous province, SW China. The extremely heavy Mg isotopic compositions of ilmenite can only result from kinetic isotope fractionation induced by Mg–Fe exchange between ilmenite and coexisting ferromagnesian silicates during the cooling of the Baima intrusion. Thus, the disequilibrium effect on cumulus minerals and rocks, which was little considered previously, should be treated seriously in investigating the petrogenesis of layered mafic intrusions.

2. Geological background and samples

The Emeishan large igneous province, derived from a ~260 Ma mantle plume, occurs in the western part of the Yangtze Block, southwest China (Fig. S1). It is predominated by widespread continental flood basalts, minor picritic lavas, and many contemporaneous mafic–ultramafic complexes and syenitic–granitic plutons (Song et al., 2001, 2008; Zhou et al., 2002; Xu et al., 2004; Zhang et al., 2006; Zhong et al., 2009). Five coeval layered mafic–ultramafic intrusions hosting world-class Fe–Ti oxide ore deposits occur in the Emeishan large igneous province central zone, namely, Taihe, Baima, Xinjie, Hongge, and Panzhihua from north to south (Panxi Geological Unit, 1984; Song et al., 2013; Chen et al., 2017). These intrusions are dated at ~260 Ma and are genetically related to the Emeishan mantle plume and the Emeishan high-Ti basaltic lavas (Zhou et al., 2002, 2008; Zhong and Zhu, 2006; Pang et al., 2008; Zhang et al., 2013).

The petrography of the Baima layered mafic intrusion (262 ± 2 Ma, Zhou et al., 2008) was presented in detail in previous studies (Panxi Geological Unit, 1984; Zhang et al., 2012, 2013; Liu et al., 2014; Chen et al., 2014; Holness et al., 2017) and is summarized briefly below. The N–S striking Baima intrusion is ~24 km long and ~1.5–6.0 km thick and dips to the west. The elongated body was surrounded by contemporaneous syenitic–granitic plutons that were emplaced into the Sinian Dengying Formation (dominated by limestone) and the Precambrian Huili group (dominated by marble and schist) (Fig. S1; Panxi Geological Unit, 1984). The Baima intrusion is characterized by medium-grained magnetite–wehrlite (Mt-wehrlite) and magnetite–troctolite (Mt-troctolite) in the Lower Zone, interlayers of fine-to-medium grained troctolite and gabbro in the Middle Zone, and fine-to-medium grained gabbro in the Upper Zone (Fig. S1; Chen et al., 2014). In addition, a few thin troctolite and gabbro are interlayered within the Mt-wehrlite and Mt-troctolite in the Lower Zone.

The Mt-wehrlite and Mt-troctolite are composed of high proportions of Fe–Ti oxides (e.g., magnetite and ilmenite, up to 70 modal%), olivine, plagioclase, and clinopyroxene, together with minor hornblende and sulfides (Fig. 1). Medium-grained ilmenite and magnetite occur as interconnected matrixes of aggregated Fe–Ti oxide grains enclosing silicates. Compared to the Mt-troctolite, the troctolite contains low contents of Fe–Ti oxides (<20%), high contents of plagioclase and olivine, as well as small abundances of clinopyroxene and hornblende. The gabbro, on the other hand, is rich in clinopyroxene and plagioclase, with <20% Fe–Ti oxide contents (Fig. 1), as well as minor olivine and/or apatite. Fine-to-medium grained and subhedral ilmenite crystals in the troctolite and gabbro are either in contact with magnetite or separated from magnetite, occurring as interstitial fillings among cumulus silicates. Micro-texture observations indicate that magnetite hosts abundant micro-intergrowths of ilmenite and hercynite while granular ilmenite has rare exsolution lamellae (Fig. 1; also see Zhang et al., 2012 and Chen et al., 2014). Moreover, both Fe–Ti oxides and silicates in the Baima intrusion are relatively fresh and little affected by post-magmatic hydrothermal alteration (e.g., Zhang et al., 2012; Chen et al., 2014).

Three Mt-wehrlites, eight Mt-troctolites, five troctolites, and four gabbros were collected from the Lower Zone and the lower part of the Middle Zone (at Jijiping segment, Fig. S1). Eleven gabbros were sampled from the upper part of the Middle Zone and the Upper Zone (the bore hole ZK42-5 at Qinggangping segment, Fig. S1). These rocks were first crushed to 120–180 μm. Fresh olivine, clinopyroxene, and ilmenite grains were then handpicked and examined under a binocular microscope at 50× magnification to a purity of approximately 100%, and finally cleaned ultrasonically three times in Milli-Q water for analysis.

3. Analytical methods

3.1. Electron probe microanalysis

Chemical compositions of ilmenite and olivine were determined on polished thin sections by an EPMA-1600 electron microprobe at the State Key Laboratory of Ore Deposit Geochemistry, Institute of Geochemistry, Chinese Academy of Sciences, with the following operating conditions: Accelerating voltage: 25 kV, beam current: 10 nA, spot diameter: 10 μm. More than five spots of ilmenite core in each section were analyzed (silicate compositions were presented in Zhang et al., 2012 and Chen et al., 2014). Besides, several detailed transects of major elements of selected ilmenite and olivine crystals were measured along directions to silicates and/or Fe–Ti oxides. Natural and synthetic oxide standards from SPI Supplies, Inc., USA, were used for data calibration.

3.2. Magnesium isotope analysis

Magnesium isotopic compositions were analyzed at the Isotope Laboratory of the University of Washington, Seattle, following a slightly modified procedure after Teng et al. (2010) and Sedaghatpour et al. (2013). Briefly, approximately 5–10 mg of pure ilmenites were dissolved in a mixture of HNO_3–HCl (~1:3) and then a concentrated HCl solution. Olivine, clinopyroxene and two international standards (DTS-1 and PCC-1) were dissolved sequentially in a mixture of concentrated HNO_3–HF (~1:3), a mixture of concentrated HNO_3–HCl (~1:3), and a concentrated HNO_3 solution. Magnesium purification for ilmenite and two international standards (DTS-1 and PCC-1) involves two steps of column chemistry (Sedaghatpour et al., 2013). The first step (i.e., Ti-column chemistry) was aimed to eliminate Ti from Mg using ion-exchange chromatography with Bio-Rad AG1-X8 resin (38–75 μm). Titanium was separated from Mg by 5 ml of 1 M HCl–0.5 M HF. The second step (i.e., Mg-column chemistry) was aimed to purify Mg from other matrix elements using Bio-Rad AG50W-X8 resin (38–75 μm) in 1 M HNO_3. Samples (after the first step) dissolved in 1 M HNO_3 were loaded on the resin and Mg was eluted in 1 M HNO_3. In contrast to ilmenite, the digested silicates as well as two international standards (DTS-1 and PCC-1, original solutions without Ti-column chemistry) were evaporated and re-dissolved in a mixture of 1 M HNO_3 and then were processed only through Mg-column chemistry as mentioned above.

The purified Mg sample solutions were measured using a Nu II MC-ICPMS in a low-resolution mode, with ^{24}Mg, ^{25}Mg, and ^{26}Mg determined simultaneously in separate Faraday cups. Magnesium isotope data are reported in δ-notation relative to the international standard DSM3: $\delta^{X}Mg$ (‰) = $[(^{X}Mg/^{24}Mg)_{sample}/(^{X}Mg/^{24}Mg)_{DSM3}-1] \times 1000$, where X refers to mass 25 or 26. The long-term external reproducibility for $\delta^{26}Mg$ is better than 0.07‰ at 2 SD level (Teng et al., 2010, 2015). Data qualities were monitored by DTS-1 and PCC-1 and two well-characterized in-house standards (SC-Ol and Seawater) processed as unknown samples in the same chemical and analytical procedures. All measured Mg isotopic data of these standards show excellent agreement with previous literature values (Table S1).

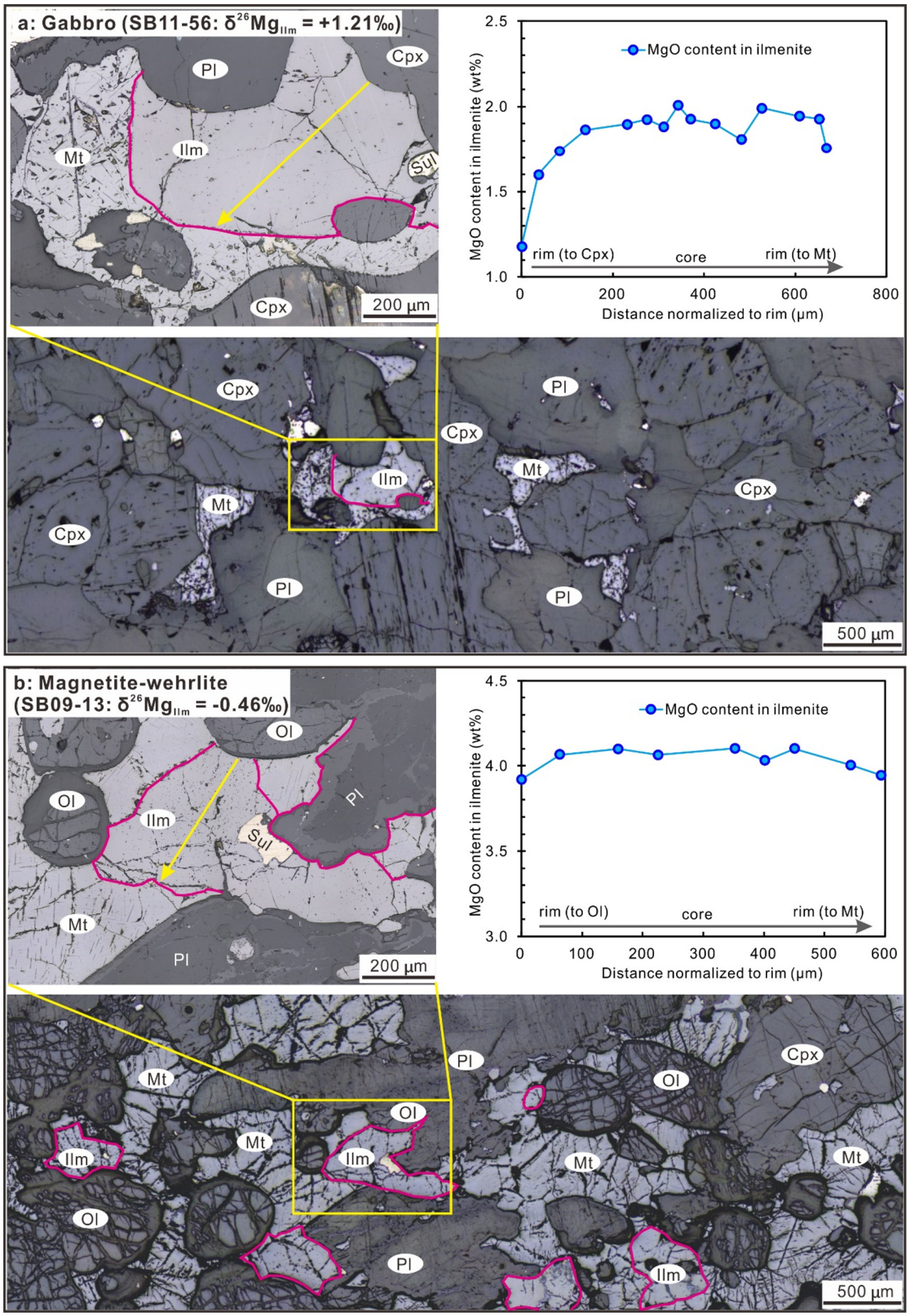

Fig. 1. (a) MgO contents in ilmenite along a traverse in the gabbro, showing decrease of MgO concentration from the core to the rim in contact with ferromagnesian silicates; (b) MgO contents in ilmenite along a traverse in the magnetite–wehrlite, showing constant MgO concentration from the core to the rim. The horizontal axis plots distance normalized to the rim in contact with ferromagnesian silicates. Abbreviations: Ol = olivine, Cpx = clinopyroxene, Pl = plagioclase, Ilm = ilmenite, Mt = magnetite, and Sul = sulfide.

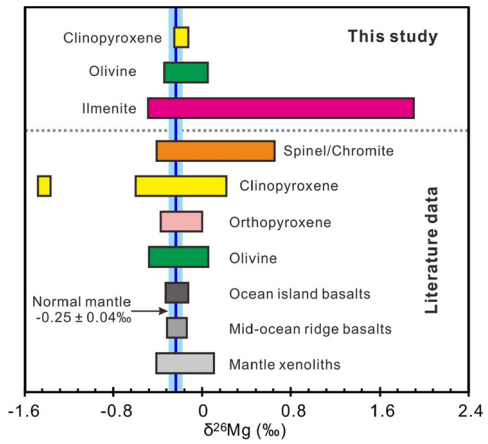

Fig. 2. Magnesium isotopic distribution in typical igneous rocks (Teng, 2017 and references therein), minerals (Yang et al., 2009; Huang et al., 2011; Liu et al., 2011; Xiao et al., 2013; Hu et al., 2016), and olivine, clinopyroxene, and ilmenite of this study. The vertical blue line and bar represent the average Mg isotopic value of the normal mantle (−0.25 ± 0.04‰, Teng et al., 2010). (For interpretation of the references to color in this figure legend, the reader is referred to the web version of this article.)

4. Results

Chemical compositions of olivine and ilmenite are reported in Table S2 and Table S3, respectively. Magnesium isotopic compositions of olivine, clinopyroxene, and ilmenite are reported in Table 1.

4.1. Chemical compositions of olivine and ilmenite

Most of olivine crystals from a single thin section have homogeneous chemical compositions except their rims adjacent to Fe–Ti oxides (Table S2), which commonly contain slightly higher forsterite contents (Fo = 100 × MgO/(MgO + FeO), in mole) than their inner parts (Fig. S2). However, four samples are exceptive. Olivine crystals from three samples (SB09-16, 28, and 30) display distinct chemical zoning with forsterite contents decreasing from core to rim (Fig. S2). Olivine grains from another sample (SB09-32), though homogeneous within individual crystals, display heterogeneous compositions among different grains (Fo = 48.2–58.8%).

Major elemental concentrations of ilmenite vary significantly in different types of rocks (Table S3). Ilmenites in the Mt-wehrlite are rich in MgO (3.74–4.56 wt%) and low in $FeO_{(T)}$ (40.2–41.4 wt%) and MnO (0.66–0.72 wt%) (Fig. S3). Ilmenites in the Mt-troctolite contains moderate MgO, $FeO_{(T)}$, and MnO contents. In addition, most of ilmenites in both Mt-wehrlite and Mt-troctolite have relatively homogeneous chemical compositions (Fig. S3), with limited elemental zoning (Fig. 1b). By contrast, ilmenites in the troctolite and gabbro are highly heterogeneous and display significant depletion of MgO (0.86–2.85 wt%) and enrichments of $FeO_{(T)}$ (43.1–46.9 wt%) and MnO (0.72–1.07 wt%) (Fig. S3). Particularly, most of ilmenites in contact with olivine and/or clinopyroxene in the troctolite and gabbro are chemically zoned, with MgO decreasing from the core to the rim (Fig. 1a), whereas ilmenites in contact with plagioclase and/or magnetite have little variation in MgO contents (Table S3).

4.2. Magnesium isotopic compositions

Olivine and clinopyroxene in all rocks display small Mg isotopic variations, with δ^{26}Mg ranging from −0.33 to −0.11‰ and from −0.29 to −0.13‰, respectively (Fig. 2), similar to silicates in mantle xenolithic peridotites (Fig. 3a), except four olivine samples of SB09-16, 28, 30, and 32. These four olivine samples, on the other hand, have elevated δ^{26}Mg values of −0.03 ± 0.05‰ and are characterized by heterogeneous chemical compositions as mentioned above (Fig. S4).

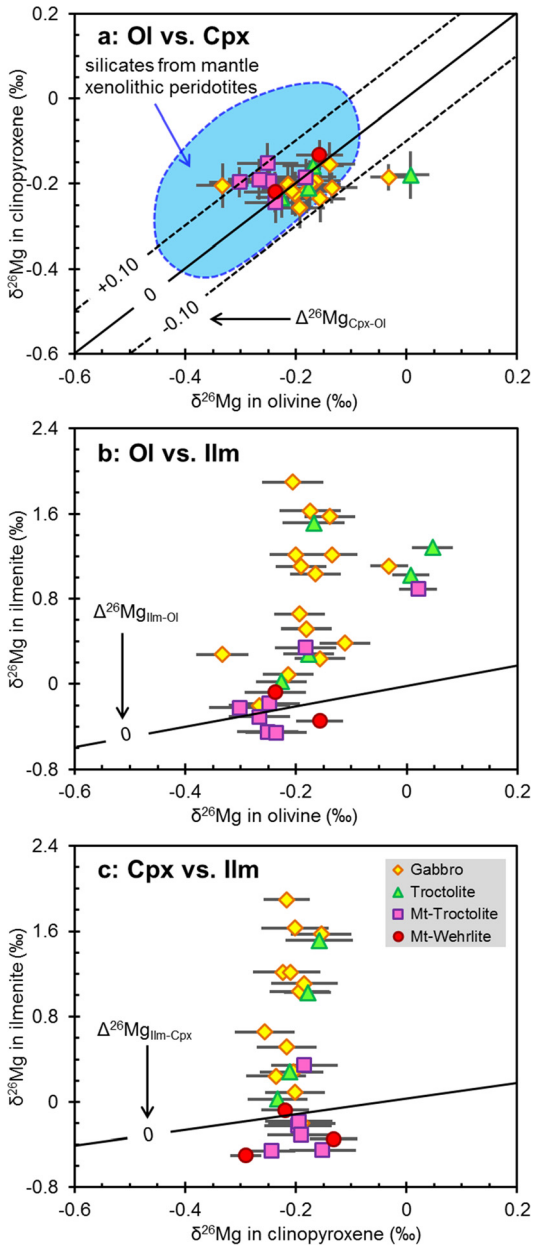

Fig. 3. Magnesium isotope fractionation (a) between olivine and clinopyroxene, (b) between olivine and ilmenite, and (c) clinopyroxene and ilmenite from the Baima intrusion. The light blue area in plot (a) represents the δ^{26}Mg of olivine and clinopyroxene from the mantle xenolithic peridotite (see reviews in Teng, 2017). Mt-wehrlite and Mt-troctolite refer to magnetite-wehrlite and magnetite-troctolite, respectively. (For interpretation of the references to color in this figure legend, the reader is referred to the web version of this article.)

Ilmenites, in contrast to olivine and clinopyroxene, display large variation in δ^{26}Mg, ranging from −0.50 to +1.90‰, which is much greater than any other igneous minerals, the normal mantle (−0.25 ± 0.04‰, Teng et al., 2010), mid-ocean ridge basalts (MORB, −0.25 ± 0.06‰), and ocean island basalts (OIB, −0.26 ± 0.08‰, Teng, 2017) worldwide (Fig. 2). More specifically, ilmenites in the Mt-wehrlite and Mt-troctolite, except three outliers (SB09-8, 16 and 27), are characterized by low δ^{26}Mg values varying from −0.50 to −0.35‰ and from −0.46 to −0.18‰, respectively. They are slightly lighter than or similar to the normal mantle in Mg isotopic compositions (Fig. 3b–c). On the other hand, ilmenites in the troctolite

Table 1
Magnesium isotopic compositions of olivine, clinopyroxene, and ilmenite (per mil) from the Baima layered mafic intrusion, Emeishan large igneous province.

Zone	Height from the base (m)	Rock type	Sample No.	Olivine				Clinopyroxene				Ilmenite			
				δ^{26}Mg	2 SD	δ^{25}Mg	2 SD	δ^{26}Mg	2 SD	δ^{25}Mg	2 SD	δ^{26}Mg	2 SD	δ^{25}Mg	2 SD
Upper Zone	1014	Apat-Gabbro	SB11−52	−0.16	0.05	−0.09	0.04	−0.24	0.05	−0.13	0.05	0.24	0.06	0.13	0.05
	997	Apat-Gabbro	SB11−58	−0.33	0.05	−0.16	0.04	−0.20	0.05	−0.10	0.05	0.28	0.05	0.11	0.04
	977	Apat-Gabbro	SB11−59	−0.18	0.05	−0.08	0.04	−0.22	0.05	−0.11	0.05	0.52	0.05	0.27	0.04
	950	Apat-Gabbro	SB11−81	−0.16	0.05	−0.07	0.04	−0.19	0.05	−0.13	0.05	1.03	0.05	0.52	0.04
	839	Apat-Ol-Gabbro	SB11−69	−0.14	0.05	−0.08	0.04	−0.15	0.05	−0.08	0.05	1.57	0.05	0.81	0.04
	820	Apat-Ol-Gabbro	SB11−68	−0.20	0.05	−0.11	0.04	−0.22	0.05	−0.11	0.05	1.21	0.05	0.63	0.04
	798	Apat-Ol-Gabbro	SB11−56	−0.14	0.05	−0.08	0.04	−0.21	0.05	−0.12	0.05	1.21	0.04	0.61	0.03
	775	Apat-Ol-Gabbro	SB11−57	−0.19	0.05	−0.12	0.04					1.10	0.05	0.52	0.04
	760	Apat-Ol-Gabbro	SB11−64	−0.11	0.05	−0.07	0.04					0.39	0.05	0.21	0.04
	740	Apat-Ol-Gabbro	SB11−65	−0.19	0.05	−0.09	0.04	−0.26	0.05	−0.14	0.05	0.66	0.05	0.33	0.04
	720	Apat-Ol-Gabbro	SB11-100	−0.21	0.05	−0.10	0.04	−0.20	0.05	−0.11	0.05	0.09	0.05	0.05	0.04
Middle Zone	680	Troctolite	SB09-39	−0.23	0.05	−0.12	0.04	−0.23	0.05	−0.12	0.05	0.02	0.05	0.03	0.04
	575	Troctolite	SB09-37	−0.18	0.05	−0.09	0.04	−0.21	0.05	−0.11	0.05	0.28	0.04	0.14	0.03
	540	Troctolite	SB09-32	0.05	0.04	0.03	0.03					1.28	0.06	0.64	0.05
	495	Ol-Gabbro	SB09-31	−0.21	0.06	−0.10	0.05	−0.22	0.04	−0.11	0.03	1.90	0.06	0.95	0.05
	465	Troctolite	SB09-30	0.01	0.03	−0.01	0.03	−0.18	0.04	−0.11	0.03	1.02	0.06	0.52	0.05
	415	Ol-Gabbro	SB09-29	−0.17	0.06	−0.09	0.05	−0.20	0.06	−0.10	0.04	1.63	0.06	0.83	0.05
	385	Ol-Gabbro	SB09-28	−0.03	0.03	−0.01	0.03	−0.18	0.06	−0.10	0.04	1.11	0.03	0.57	0.03
Lower Zone	355	Mt-Troctolite	SB09-27	−0.18	0.06	−0.09	0.05	−0.18	0.06	−0.11	0.04	0.35	0.04	0.19	0.04
	325	Mt-Troctolite	SB09-25	−0.30	0.06	−0.15	0.05	−0.20	0.06	−0.09	0.04	−0.22	0.04	−0.12	0.03
	295	Troctolite	SB09-24	−0.17	0.06	−0.08	0.05	−0.16	0.06	−0.06	0.04	1.51	0.04	0.78	0.03
	266	Ol-Gabbro	SB09-20	−0.27	0.06	−0.14	0.05	−0.19	0.06	−0.07	0.04	−0.20	0.05	−0.08	0.04
	216	Mt-Troctolite	SB09-19	−0.25	0.06	−0.11	0.05	−0.19	0.06	−0.09	0.04	−0.18	0.05	−0.09	0.04
	202	Mt-Troctolite	SB09-18	−0.25	0.06	−0.13	0.05	−0.15	0.06	−0.08	0.04	−0.45	0.05	−0.23	0.04
	192	Mt-Troctolite	SB09-17	−0.27	0.06	−0.14	0.05	−0.19	0.06	−0.10	0.04	−0.31	0.05	−0.14	0.04
	182	Mt-Troctolite	SB09-16	0.02	0.03	0.02	0.03					0.89	0.05	0.45	0.04
	157	Mt-Wehrlite	SB09-15					−0.29	0.03	−0.15	0.02	−0.50	0.05	−0.26	0.04
	137	Mt-Wehrlite	SB09-14	−0.21	0.06	−0.09	0.05								
	113	Mt-Troctolite	SB09-13	−0.24	0.06	−0.11	0.05	−0.24	0.04	−0.13	0.04	−0.46	0.05	−0.23	0.04
	102	Mt-Wehrlite	SB09-11	−0.16	0.04	−0.09	0.03	−0.13	0.04	−0.07	0.04	−0.35	0.04	−0.17	0.03
	60	Mt-Wehrlite	SB09-08	−0.24	0.06	−0.13	0.05	−0.22	0.04	−0.11	0.04	−0.08	0.05	−0.03	0.04

All data were analyzed on a Nu Plasma II MC-ICP-MS at the Isotope Laboratory of the University of Washington, Seattle.
2 SD refers to 2 times standard deviation of the population of n ($n > 20$) repeated analyses of the standards during an analytical session.
Some numbers are the average values and their associated 2 SD, which are calculated from error-weighted values. See Table S4 for individual analyses.
Abbreviations: Mt-Wehrlite = magnetite wehrlite; Mt-Troctlite = magnetite troctlite; Ol-Gabbro = olivine gabbro; Apat-Ol-Gabbro = apatite olivine gabrro; Apat-Gabbro = apatite gabrro.

and gabbro (except one sample of SB09-20) show very heavy Mg isotopic compositions, with δ^{26}Mg ranging from +0.02 to +1.51‰ and from +0.09 to +1.90‰, respectively. They are much heavier than the normal mantle and those in the Mt-wehrlite and Mt-troctolite in Mg isotopic compositions (Fig. 3b–c).

5. Discussion

Petrological and geochemical investigations have indicated that olivine, clinopyroxene, ilmenite, and magnetite of the Baima intrusion co-crystallized from evolved Fe–Ti-enriched basaltic magmas in the Baima magma chamber (Zhang et al., 2012; Chen et al., 2014; Liu et al., 2014). Therefore, Mg isotopic variations in these cumulus minerals may result from inter-mineral equilibrium fractionation and/or kinetic isotope fractionation. Below, we first discuss the detailed mechanisms and geological processes governing Mg isotopic variations in these minerals during magmatic processes. Then, we explore their potential petrologic implications.

5.1. Equilibrium Mg isotope fractionation

Equilibrium Mg isotope fractionation depends on the bonding environment of Mg, with heavier isotopes preferring stronger bonds (i.e., lower coordination polyhedron) (Bigeleisen and Mayer, 1947; Liu et al., 2011; Schauble, 2011; Huang et al., 2013). Since Mg in olivine and clinopyroxene has similar bonding environment, Mg isotope fractionation between them is expected to be limited ($\leq$0.1‰) at magmatic temperatures. This expectation has been predicated by theoretical consideration (Liu et al., 2011; Schauble, 2011) and evidenced by studies of mantle xenoliths (Handler et al., 2009; Yang et al., 2009; Huang et al., 2011; Liu et al., 2011; Hu et al., 2016). Indeed, except four olivine samples with elevated δ^{26}Mg values, all silicates have $\Delta^{26}Mg_{Cpx-Ol}$ values ($\Delta^{26}Mg_{Cpx-Ol} = \delta^{26}Mg_{Cpx} - \delta^{26}Mg_{Ol}$) between −0.10 and +0.10‰ (Fig. 3a). Therefore, such observations suggest an equilibrium Mg isotope fractionation between olivine and clinopyroxene for most of the Baima rocks. However, other four olivine samples have much heavier Mg isotopic compositions than coexisting clinopyroxene with $\Delta^{26}Mg_{Cpx-Ol}$ varying from −0.19 to −0.15‰, indicating disequilibrium fractionation (Table 1).

A possible explanation for the slightly elevated δ^{26}Mg values (−0.03–+0.05‰) of four olivines is that they fractionated from newly injected magmas with heavy Mg isotope compositions. Previous studies have indicated that the Baima parental magmas had experienced crystallization of silicates and Cr-rich spinel in deep-seated magma chambers (Zhang et al., 2012; Chen et al., 2014). However, crystallization of silicates can hardly shift Mg isotopic composition of the residual magma (Teng et al., 2007, 2011); and crystallization of spinel should have lowered Mg isotopic composition of the residual magma (Fig. S5). This is because spinel is isotopically heavier than coexisting silicates under equilibrium fractionation (Liu et al., 2011; Su et al., 2017). The direct evidence against this hypothesis comes from a recent study that shows the Emeishan high-Ti basalts, which are genetically related to the Baima mafic layered intrusion (e.g., Zhou et al., 2008; Zhang et al., 2012, 2013), have similar Mg isotopic compositions (δ^{26}Mg = −0.35–−0.19‰, with a mean of −0.25 ± 0.09‰) to the clinopyroxenes and most olivines in the Baima intrusion (Tian et al., 2017). Consequently, given the chemical heterogeneities of these olivine samples (Fig. S4), their elevated δ^{26}Mg values could be attributed to kinetic fractionation caused by Mg–Fe inter-diffusion between olivine and residual melts.

The inter-mineral fractionation of Mg isotopes involving ilmenite reflects both equilibrium and kinetic processes. To date, neither a reduced isotopic partition function ratio (i.e., β-factor) of Mg isotopes for ilmenite nor an equilibrium Mg isotopic fractionation factor between ilmenite and melt has been quantitatively estimated. Nonetheless, given two observations: (1) β-factors of Mg isotopes are theoretically consistent with those of Fe isotopes in Fe(II)-bearing species (Schauble, 2011) and (2) β-factors of Fe isotopes in ilmenite are smaller than those in ferromagnesian silicates (Polyakov and Mineev, 2000; Chen et al., 2014; Sossi and O'Neill, 2017), it is likely that ilmenite has a lower β-factor of Mg isotopes than olivine and clinopyroxene. Indeed, in this study, five ilmenites in the Mt-wehrlite and Mt-troctolite are isotopically lighter than the coexisting olivine and clinopyroxene with $\Delta^{26}Mg_{Ilm-Ol}$ and $\Delta^{26}Mg_{Ilm-Cpx}$ varying from −0.04 to −0.22‰ and from −0.12 to −0.30‰ (Fig. 3b–c), respectively. In addition, these five ilmenites contain the highest MgO concentrations (3.60–4.56 wt%) than other ilmenites (Fig. S3) and do not display any chemical zoning (Table S3). Therefore, the inter-mineral Mg isotope fractionation between these five ilmenites and coexisting silicates could be the best estimates for equilibrium fractionation. By contrast, the rest of ilmenite containing lower MgO concentrations has much heavier Mg isotopic compositions than coexisting olivine and clinopyroxene with $\Delta^{26}Mg_{Ilm-Ol}$ and $\Delta^{26}Mg_{Ilm-Cpx}$ ranging from +0.07 to +2.11‰ and from 0 to +2.22‰ (Fig. 3b–c), respectively. The heavy Mg isotopic compositions in these ilmenites could not be ascribed to post-magmatic hydrothermal alteration, because all measured samples are quite fresh as evidenced by their micro texture (Fig. 1). Moreover, the δ^{26}Mg values of these ilmenites do not correlate with loss on ignition of whole rocks (Fig. S6), further indicating that hydrothermal alteration played negligible role on Mg isotope variation. Instead, they are strongly indicative of kinetic Mg isotope fractionation, which will be discussed in detail below.

5.2. Diffusion-driven kinetic magnesium isotope fractionation

Recent studies have found large Mg kinetic isotope fractionation produced by thermal diffusion and chemical diffusion (Teng, 2017 and references therein). Thermal diffusion could produce large Mg isotope fractionation, with heavy Mg isotopes preferentially enriched at the cold end (Richter et al., 2008, 2009; Huang et al., 2010). However, thermal diffusion cannot be responsible for the heavy Mg isotopic compositions in ilmenite because of the 8–12 orders of magnitude faster diffusivity of heat (Lesher and Walker, 1986) than that of Mg–Fe in Fe–Ti oxides (Van Orman and Crispin, 2010) at magmatic temperatures (e.g., 1100 °C). It is speculated that no measurable temperature gradient can occur at the grain scale either. Alternatively, the coupled correlations between Mg isotopes and elemental compositions indicate that the heavy Mg isotopic compositions in ilmenite were primarily produced by kinetic fractionation induced by chemical diffusion (Fig. 4). This interpretation is further supported by the large intra- and inter-grain chemical heterogeneities (Figs. 1a, 4), indicating chemical disequilibrium. Furthermore, given the fast diffusivity of Mg–Fe in ilmenite at magmatic temperatures (Van Orman and Crispin, 2010), Mg isotope variation in ilmenites likely resulted from inter-mineral diffusion between ilmenites and ferromagnesian silicates during subsolidus processes.

Experimental studies have demonstrated that concentration of MgO in ilmenite would decrease with temperature during crystallization (Fig. S7, Toplis and Carroll, 1995). Therefore, if ilmenite crystallized at high temperature re-equilibrates at relatively low temperature, its MgO would diffuse out during cooling. Mineral textures and Fe isotopic investigations have revealed that Fe–Ti oxides and ferromagnesian silicates had experienced chemical exchange at subsolidus temperatures in the Baima layered intrusion (Chen et al., 2014). During subsolidus processes, Mg^{2+} would diffuse from ilmenite into coexisting ferromagnesian silicates (i.e.,

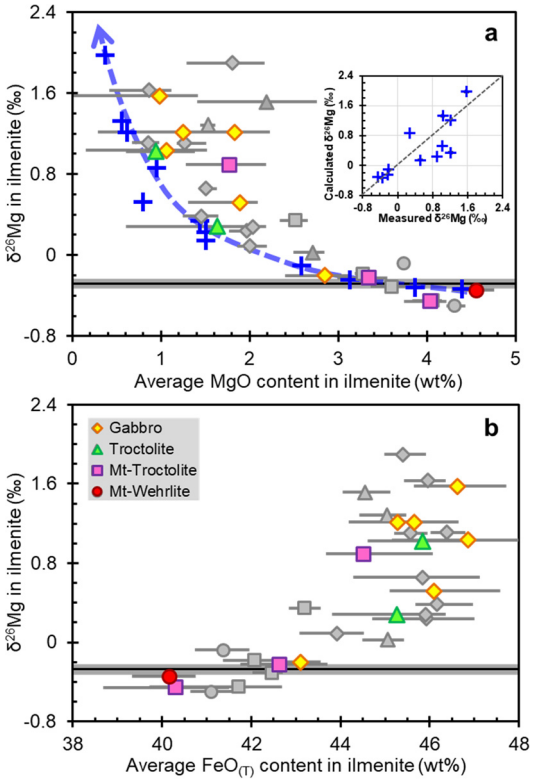

Fig. 4. (a) Binary plot and quantitative model for δ^{26}Mg values vs. MgO concentrations in ilmenites. Twelve ilmenite samples with core and rim MgO content measured, as highlighted by the colorful fills, have been used for the diffusion modeling. The model results are shown as blue crosses. The light-blue dash line represents a trend of δ^{26}Mg vs. MgO for these 12 samples. The modeled δ^{26}Mg vs. the measured value is also plotted in the inserted figure. The overall correlation between the modeled δ^{26}Mg vs. the measured δ^{26}Mg is better than that between δ^{26}Mg vs. MgO. This is because the modeled δ^{26}Mg is predominately determined by the β-factor while the modeled MgO content depends on several assumptions (e.g., an ilmenite crystal has to be a sphere). Furthermore, the average MgO content of the ilmenite may not represent the true average either as most ilmenite data are from the core, which tends to have higher MgO than the rim. The rock types of those samples with gray fills are indicated by the same symbol shape as these 12 samples. (b) Binary plot for δ^{26}Mg values vs. $FeO_{(T)}$ concentrations in ilmenites. Error bars of Mg isotopes are smaller than the sizes of the symbols, and error bars of MgO and $FeO_{(T)}$ contents represent the abundance range measured in this study. The horizontal black line and gray bar in both panels represent the average Mg isotopic value of the normal mantle (-0.25 ± 0.04‰, Teng et al., 2010). (For interpretation of the references to color in this figure legend, the reader is referred to the web version of this article.)

olivine and clinopyroxene) in which Mg^{2+} is more compatible during cooling, engendering the former to be depleted in MgO/FeO ratios (Morse, 1980; Pang et al., 2008; Chen et al., 2017). In-situ analyses of chemical profiles reveal that most of ilmenites in the troctolite and gabbro contain MgO contents decreasing from the core to the rim in contact with olivine and clinopyroxene (Figs. 1a, S3). This chemical exchange would elevate δ^{26}Mg values in ilmenites, due to the faster diffusivity of light Mg isotopes (e.g., ^{24}Mg) than the heavier one (i.e., ^{26}Mg) (Richter et al., 2008, 2009). Furthermore, the magnitude of the subsolidus exchange between minerals depends on cumulus mineral modal proportions and elemental concentration because of dilution effects (Chen et al., 2014; Xiao et al., 2016). Consequently, chemical exchange of ilmenite in the Mt-wehrlite and Mt-troctolite were much less extensive than those in the troctolite and gabbro because ilmenite abundance in the former rocks is higher than that in the later ones. This interpretation is further supported by the negative correlations of δ^{26}Mg values of ilmenite with TiO_2 of bulk rocks (Fig. 5). By contrast, although both olivine and clinopyroxene were inevitably affected by subsolidus chemical exchange, their Mg isotopic compositions had been little affected because of their high MgO concentrations and high modal proportions in the Baima cumulate rocks.

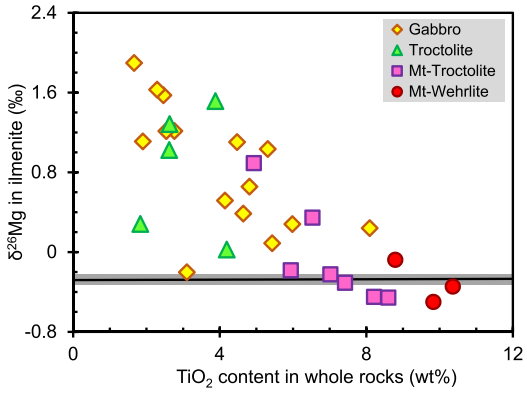

Fig. 5. Binary plots for δ^{26}Mg values in ilmenites vs. TiO_2 contents in whole rocks (TiO_2 values are from Chen et al., 2014). Error bars of Mg isotopes are smaller than the sizes of the symbols. The horizontal black line and gray bar represent the average Mg isotopic value of the normal mantle (-0.25 ± 0.04‰, Teng et al., 2010).

Magnesium isotope fractionation induced by chemical diffusion can be further quantitatively modeled as follows. Under a concentration gradient, the diffusive fractionation of Mg isotopes between the high and low concentration ends ($\Delta Mg_{High-Low}$) is calculated using the diffusion-theory-based model deduced from Fick's first law (Zhu et al., 2015):

$$\Delta Mg_{High-Low}(‰) = 1000 \times \left[1 - (m_2/m_1)^{\beta})\right] \times (1 - C_{Low}/C_{High}) \quad (1)$$

where m_1 and m_2 are masses of heavy and light isotopes, i.e., 26 and 24, respectively; C_{High} and C_{Low} are MgO concentrations in the high and low concentration ends, respectively; β is an empirical parameter that depends on the diffusion medium. Moreover, the bulk chemical composition (C_{bulk}) and isotopic composition (δ_{bulk}) of one sample, which is assumed to be a sphere, are given by:

$$C_{bulk} = \int_0^R 4\pi C(r) r^2 dr \Big/ \int_0^R 4\pi r^2 dr \quad (2)$$

$$\delta_{bulk} = \int_0^R 4\pi \delta(r) C(r) r^2 dr \Big/ \int_0^R 4\pi C(r) r^2 dr \quad (3)$$

In the model calculations, δ^{26}Mg value of the low concentration end (i.e., rim) in ilmenite is assumed to be -0.50‰, which represents Mg isotopic compositions in equilibrium fractionation as discussed in section 5.1. The β value for ilmenite is estimated by fitting the measured data to be 0.08, which is within the range of those measured in liquid silicates (0.05–0.10, Richter et al., 2009; Watkins et al., 2011; Oeser et al., 2015). The model results are well consistent with the measured chemical and isotopic compositions in ilmenite (Fig. 4a), further confirming their heavy Mg isotopic compositions were produced by diffusion-driven kinetic isotope fractionation.

5.3. Petrologic implications

The large Mg isotope fractionation observed between these cumulus minerals provides critical insight into the light Mg isotopic compositions of lunar high-Ti basalts and the widespread disequilibrium fractionation during magmatic processes. These geological implications are evaluated below.

5.3.1. Implication on light Mg isotopic compositions of lunar high-Ti basalts

Lunar mare basalts originated from partial melting of the Moon's deep interior, which was compositionally stratified due to differentiation of the lunar magma ocean (Grove and Krawczynski, 2009). The source of the lunar basalts, particularly the high-Ti basalts, was proposed to be related to ilmenite-bearing zones, which could result from either sinking of ilmenite-rich cumulates into the lunar mantle due to gravitational instabilities or assimilation of late-stage ilmenite-rich cumulates during magma ascent (e.g., Hess and Parmentier, 1995; Wagner and Grove, 1997). Therefore, ilmenites and their geochemical features are important for understanding the petrogenesis of the lunar mare basalts.

Sedaghatpour et al. (2013) found that the lunar high-Ti basalts were characterized by light Mg isotopic compositions (δ^{26}Mg = −0.61–−0.33‰) relative to the low-Ti ones (δ^{26}Mg = −0.34–−0.02‰), though the bulk moon had an average Mg isotopic composition (δ^{26}Mg = −0.26 ± 0.16‰) indistinguishable from the Earth. Based on the positive correlations between δ^{26}Mg and TiO_2 in bulk rocks, they suggested that the high-Ti basalts may originate from an isotopically light source enriched in cumulate ilmenites, which were speculated to have lighter Mg isotopic compositions than coexisting olivine and pyroxene.

Our study provides a strong constraint on the above interpretation. Indeed, five ilmenite samples (δ^{26}Mg = −0.50–−0.31‰) are isotopically lighter than coexisting olivine and pyroxene at near equilibrium conditions (Fig. 3b–c), verifying the above speculation. Moreover, the planet-wide magmatic system, e.g., the lunar magma ocean, has a million-year scale of cooling history (Shearer et al., 2006), which would give rise to an equilibrium isotope fractionation for ilmenite during solidification of the lunar magma ocean. Therefore, partial melting of ilmenite-bearing cumulates with light Mg isotopic compositions in the mantle source could produce isotopically light lunar high-Ti basalts. This proposal is well consistent with the hypothesis of the lunar magma ocean (Walker et al., 1975). Nonetheless, terrestrial ilmenite cumulates might be different from those in the lunar magma ocean, hence direct analysis of lunar ilmenite is required to further explore the role of ilmenite cumulates in producing the isotopically light lunar high-Ti basalts.

5.3.2. Widespread disequilibrium fractionation during magmatic processes

Chemical compositions of cumulus minerals in magma chambers have been commonly presumed to achieve thermodynamic equilibrium on studies of petrogenesis of mafic–ultramafic rocks. However, the chemical diffusion-induced kinetic Mg isotope fractionation between Fe–Ti oxides and coexisting silicates, together with elemental zoning in ilmenite and olivine (Figs. 1a, S2), implies the compositional disequilibrium among cumulus minerals in the Baima layered mafic intrusion.

Globally, kinetic Mg isotope fractionation caused by chemical diffusion appears to be an important and widespread mechanism for producing "unique" Mg isotopic signatures during magmatic processes. Large Mg isotope fractionation produced by chemical diffusion has been found in igneous minerals and bulk samples from mantle xenoliths (Xiao et al., 2013; Hu et al., 2016), ophiolite (Xiao et al., 2016), volcanic lavas (Teng et al., 2011; Sio et al., 2013; Oeser et al., 2015), and felsic and mafic rocks (Pogge von Strandmann et al., 2015; Wu et al., 2017). Similarly, kinetic isotope fractionations have been observed widely in other non-traditional stable isotope systems during magmatic processes, such as Fe and Li isotopes (see reviews in Dauphas et al., 2017 and Penniston-Dorland et al., 2017, respectively). The preservation of kinetic isotope fractionation further demonstrates the widespread compositional disequilibrium in igneous minerals and rocks. These results challenge the long-standing view that the coexisting igneous minerals in cumulate rocks are in thermodynamic equilibrium owing to fast diffusivities of elements during magmatic processes. Therefore, the reliabilities of using chemical compositions in cumulus minerals to estimate magmatic differentiation, magma chamber processes, and magmatic oxide ore genesis as were often done in studies of layered mafic intrusions, require rigorous reassessment.

6. Conclusions

Magnesium isotopic compositions of olivine, clinopyroxene, and ilmenite from the Baima layered mafic intrusion, SW China, have been investigated in this study. Olivine and clinopyroxene display small Mg isotopic variations, whereas ilmenites are characterized by extremely large Mg isotope fractionation. Most of olivine, all clinopyroxene, and a few of ilmenite were in Mg isotope equilibrium, where ilmenites were isotopically lighter than coexisting silicates. These observations imply that the light Mg isotopic compositions of lunar high-Ti basalts are caused by cumulate ilmenites in their source. By contrast, the very heavy Mg isotopic compositions of most of ilmenites were attributed to kinetic isotope fractionation induced by subsolidus Mg–Fe exchange between ilmenite and ferromagnesian silicates during the fast cooling of the Baima intrusion. The large kinetic Mg isotope fractionation indicates the widespread compositional disequilibrium in igneous minerals and rocks. Consequently, the disequilibrium effects need to be considered seriously before applying mineral compositions to constrain petrogenesis of layered mafic intrusions.

Acknowledgements

This study is supported by the NSFC (41473024, 41573009, and 41530210), the National Key Research and Development Program of China (2016YFC0600503), the Strategic Priority Research Program (B) of the Chinese Academy of Sciences (XDB18000000), and NSF (EAR-17407706). We are grateful to Zhe Yang, Yang Sun, Yan Hu, and Jin-Long Ma for their help on Mg isotope analysis, and Wen-Qin Zheng for her effort in EPMA analysis. We greatly appreciate three anonymous reviewers for their constructive and detailed reviews, and Prof. Frederic Moynier for his efficient editorial handling. Jia-Fei Zhang is thanked for his assistance during the fieldwork.

Appendix A. Supplementary material

Supplementary material related to this article can be found online at https://doi.org/10.1016/j.epsl.2018.01.036.

References

Bigeleisen, J., Mayer, M.G., 1947. Calculation of equilibrium constants for isotopic exchange reactions. J. Chem. Phys. 15, 261–267.

Chen, L.-M., Song, X.-Y., Hu, R.-Z., Yu, S.-Y., He, H.-L., Dai, Z.-H., She, Y.-W., Xie, W., 2017. Controls on trace-element partitioning among co-crystallizing minerals: evidence from the Panzhihua layered intrusion, SW China. Am. Mineral. 102, 1006–1020.

Chen, L.-M., Song, X.-Y., Zhu, X.-K., Zhang, X.-Q., Yu, S.-Y., Yi, J.-N., 2014. Iron isotope fractionation during crystallization and sub-solidus re-equilibration: constraints from the Baima mafic layered intrusion, SW China. Chem. Geol. 380, 97–109.

Chopra, R., Richter, F.M., Bruce Watson, E., Scullard, C.R., 2012. Magnesium isotope fractionation by chemical diffusion in natural settings and in laboratory analogues. Geochim. Cosmochim. Acta 88, 1–18.

Collinet, M., Charlier, B., Namur, O., Oeser, M., Médard, E., Weyer, S., 2017. Crystallization history of enriched shergottites from Fe and Mg isotope fractionation in olivine megacrysts. Geochim. Cosmochim. Acta 207, 277–297.

Dauphas, N., John, S.G., Rouxel, O., 2017. Iron isotope systematics. Rev. Mineral. Geochem. 82, 415–510.

Grove, T.L., Krawczynski, M.J., 2009. Lunar mare volcanism: where did the magmas come from? Elements 5, 29–34.

Handler, M.R., Baker, J.A., Schiller, M., Bennett, V.C., Yaxley, G.M., 2009. Magnesium stable isotope composition of Earth's upper mantle. Earth Planet. Sci. Lett. 282, 306–313.
Hess, P.C., Parmentier, E.M., 1995. A model for the thermal and chemical evolution of the Moon's interior: implications for the onset of mare volcanism. Earth Planet. Sci. Lett. 134, 501–514.
Holness, M.B., Vukmanovic, Z., Mariani, E., 2017. Assessing the role of compaction in the formation of adcumulates: a microstructural perspective. J. Petrol. 58, 643–673.
Hu, Y., Teng, F.-Z., Zhang, H.-F., Xiao, Y., Su, B.-X., 2016. Metasomatism-induced mantle magnesium isotopic heterogeneity: evidence from pyroxenites. Geochim. Cosmochim. Acta 185, 88–111.
Huang, F., Chakraborty, P., Lundstrom, C.C., Holmden, C., Glessner, J.J.G., Kieffer, S.W., Lesher, C.E., 2010. Isotope fractionation in silicate melts by thermal diffusion. Nature 464, 396–400.
Huang, F., Chen, L., Wu, Z., Wang, W., 2013. First-principles calculations of equilibrium Mg isotope fractionations between garnet, clinopyroxene, orthopyroxene, and olivine: implications for Mg isotope thermometry. Earth Planet. Sci. Lett. 367, 61–70.
Huang, F., Zhang, Z.F., Lundstrom, C.C., Zhi, X.C., 2011. Iron and magnesium isotopic compositions of peridotite xenoliths from Eastern China. Geochim. Cosmochim. Acta 75, 3318–3334.
Lesher, C.E., Walker, D., 1986. Solution properties of silicate liquids from thermal diffusion experiments. Geochim. Cosmochim. Acta 50, 1397–1411.
Liu, P.-P., Zhou, M.-F., Wang, C.Y., Xing, C.-M., Gao, J.-F., 2014. Open magma chamber processes in the formation of the Permian Baima mafic–ultramafic layered intrusion, SW China. Lithos 184–187, 194–208.
Liu, S.-A., Teng, F.-Z., Yang, W., Wu, F.-Y., 2011. High-temperature inter-mineral magnesium isotope fractionation in mantle xenoliths from the North China craton. Earth Planet. Sci. Lett. 308, 131–140.
Morse, S.A., 1980. Kiglapait mineralogy II: Fe–Ti oxide minerals and the activities of oxygen and silica. J. Petrol. 21, 685–719.
Namur, O., Abily, B., Boudreau, A.E., Blanchette, F., Bush, J.W.M., Ceuleneer, G., Charlier, B., Donaldson, C.H., Duchesne, J.-C., Higgins, M.D., Morata, D., Nielsen, T.F.D., O'Driscoll, B., Pang, K.N., Peacock, T., Spandler, C.J., Toramaru, A., Veksler, I.V., 2015. Igneous layering in basaltic magma chambers. In: Charlier, B., Namur, O., Latypov, R., Tegner, C. (Eds.), Layered Intrusions. Springer, Netherlands, Dordrecht, pp. 75–152.
Oeser, M., Dohmen, R., Horn, I., Schuth, S., Weyer, S., 2015. Processes and time scales of magmatic evolution as revealed by Fe–Mg chemical and isotopic zoning in natural olivines. Geochim. Cosmochim. Acta 154, 130–150.
Pang, K.N., Zhou, M.F., Lindsley, D., Zhao, D., Malpas, J., 2008. Origin of Fe–Ti oxide ores in mafic intrusions: evidence from the Panzhihua intrusion, SW China. J. Petrol. 49, 295–313.
Panxi Geological Unit, 1984. Mineralization and Exploration Forecasting of V–Ti Magnetite Deposits in the Panzhihua–Xichang Region. pp. 279 (in Chinese).
Penniston-Dorland, S., Liu, X.-M., Rudnick, R.L., 2017. Lithium isotope geochemistry. Rev. Mineral. Geochem. 82, 165–217.
Pogge von Strandmann, P.A.E., Dohmen, R., Marschall, H.R., Schumacher, J.C., Elliott, T., 2015. Extreme magnesium isotope fractionation at outcrop scale records the mechanism and rate at which reaction fronts advance. J. Petrol. 56, 33–58.
Polyakov, V.B., Mineev, S.D., 2000. The use of Mössbauer spectroscopy in stable isotope geochemistry. Geochim. Cosmochim. Acta 64, 849–865.
Richter, F., Chaussidon, M., Mendybaev, R., Kite, E., 2016. Reassessing the cooling rate and geologic setting of Martian meteorites MIL 03346 and NWA 817. Geochim. Cosmochim. Acta 182, 1–23.
Richter, F.M., Watson, E.B., Mendybaev, R., Dauphas, N., Georg, B., Watkins, J., Valley, J., 2009. Isotopic fractionation of the major elements of molten basalt by chemical and thermal diffusion. Geochim. Cosmochim. Acta 73, 4250–4263.
Richter, F.M., Watson, E.B., Mendybaev, R.A., Teng, F.Z., Janney, P.E., 2008. Magnesium isotope fractionation in silicate melts by chemical and thermal diffusion. Geochim. Cosmochim. Acta 72, 206–220.
Schauble, E.A., 2011. First-principles estimates of equilibrium magnesium isotope fractionation in silicate, oxide, carbonate and hexaaquamagnesium(2+) crystals. Geochim. Cosmochim. Acta 75, 844–869.
Shearer, C.K., Hess, P.C., Wieczorek, M.A., Pritchard, M.E., Parmentier, E.M., Borg, L.E., Longhi, J., Elkins-Tanton, L.T., Neal, C.R., Antonenko, I., Canup, R.M., Halliday, A.N., Grove, T.L., Hager, B.H., Lee, D.-C., Wiechert, U., 2006. Thermal and magmatic evolution of the Moon. Rev. Mineral. Geochem. 60, 365–518.
Scoates, J.S., Wall, C.J., 2015. Geochronology of layered intrusions. In: Charlier, B., Namur, O., Latypov, R., Tegner, C. (Eds.), Layered Intrusions. Springer, Netherlands, Dordrecht, pp. 3–74.
Sedaghatpour, F., Teng, F.-Z., Liu, Y., Sears, D.W.G., Taylor, L.A., 2013. Magnesium isotopic composition of the Moon. Geochim. Cosmochim. Acta 120, 1–16.
Sio, C.K.I., Dauphas, N., Teng, F.-Z., Chaussidon, M., Helz, R.T., Roskosz, M., 2013. Discerning crystal growth from diffusion profiles in zoned olivine by in situ Mg–Fe isotopic analyses. Geochim. Cosmochim. Acta 123, 302–321.
Song, X.Y., Qi, H.W., Hu, R.Z., Chen, L.M., Yu, S.Y., Zhang, J.F., 2013. Formation of thick stratiform Fe–Ti oxide layers in layered intrusion and frequent replenishment of fractionated mafic magma: evidence from the Panzhihua intrusion, SW China. Geochem. Geophys. Geosyst. 14, 712–732.
Song, X.Y., Qi, H.W., Robinson, P.T., Zhou, M.F., Cao, Z.M., Chen, L.M., 2008. Melting of the subcontinental lithospheric mantle by the Emeishan mantle plume; evidence from the basal alkaline basalts in Dongchuan, Yunnan, Southwestern China. Lithos 100, 93–111.
Song, X.Y., Zhou, M.F., Hou, Z.Q., Cao, Z.M., Wang, Y.L., Li, Y.G., 2001. Geochemical constraints on the mantle source of the upper permian Emeishan continental flood basalts, southwestern China. Int. Geol. Rev. 43, 213–225.
Sossi, P.A., O'Neill, H.S.C., 2017. The effect of bonding environment on iron isotope fractionation between minerals at high temperature. Geochim. Cosmochim. Acta 196, 121–143.
Su, B.-X., Hu, Y., Teng, F.-Z., Qin, K.-Z., Bai, Y., Sakyi, P.A., Tang, D.-M., 2017. Chromite-induced magnesium isotope fractionation during mafic magma differentiation. Sci. Bull. 62, 1538–1546.
Tian, H.-C., Yang, W., Li, S.-G., Ke, S., 2017. Could sedimentary carbonates be recycled into the lower mantle? Constraints from Mg isotopic composition of Emeishan basalts. Lithos 292–293, 250–261.
Teng, F.-Z., 2017. Magnesium isotope geochemistry. Rev. Mineral. Geochem. 82, 219–287.
Teng, F.-Z., Dauphas, N., Helz, R.T., Gao, S., Huang, S., 2011. Diffusion-driven magnesium and iron isotope fractionation in Hawaiian olivine. Earth Planet. Sci. Lett. 308, 317–324.
Teng, F.-Z., Li, W.-Y., Ke, S., Marty, B., Dauphas, N., Huang, S., Wu, F.-Y., Pourmand, A., 2010. Magnesium isotopic composition of the Earth and chondrites. Geochim. Cosmochim. Acta 74, 4150–4166.
Teng, F.-Z., Li, W.-Y., Ke, S., Yang, W., Liu, S.-A., Sedaghatpour, F., Wang, S.-J., Huang, K.-J., Hu, Y., Ling, M.-X., Xiao, Y., Liu, X.-M., Li, X.-W., Gu, H.-O., Sio, C.K., Wallace, D.A., Su, B.-X., Zhao, L., Chamberlin, J., Harrington, M., Brewer, A., 2015. Magnesium isotopic compositions of international geological reference materials. Geostand. Geoanal. Res. 39, 329–339.
Teng, F.-Z., Wadhwa, M., Helz, R.T., 2007. Investigation of magnesium isotope fractionation during basalt differentiation: implications for a chondritic composition of the terrestrial mantle. Earth Planet. Sci. Lett. 261, 84–92.
Toplis, M.J., Carroll, M.R., 1995. An experimental study of the influence of oxygen fugacity on Fe–Ti oxide stability, phase relations, and mineral-melt equilibria in ferro–basaltic systems. J. Petrol. 36, 1137–1170.
Van Orman, J.A., Crispin, K.L., 2010. Diffusion in oxides. Rev. Mineral. Geochem. 72, 757–825.
Wagner, T.P., Grove, T.L., 1997. Experimental constraints on the origin of lunar high-Ti ultramafic glasses. Geochim. Cosmochim. Acta 61, 1315–1327.
Walker, D., Longhi, J., Stolper, E.M., Grove, T.L., Hays, J.F., 1975. Origin of titaniferous lunar basalts. Geochim. Cosmochim. Acta 39, 1219–1235.
Watkins, J.M., DePaolo, D.J., Ryerson, F.J., Peterson, B.T., 2011. Influence of liquid structure on diffusive isotope separation in molten silicates and aqueous solutions. Geochim. Cosmochim. Acta 75, 3103–3118.
Wu, H., He, Y., Bao, L., Zhu, C., Li, S., 2017. Mineral composition control on inter-mineral iron isotopic fractionation in granitoids. Geochim. Cosmochim. Acta 198, 208–217.
Xiao, Y., Teng, F.-Z., Su, B.-X., Hu, Y., Zhou, M.-F., Zhu, B., Shi, R.-D., Huang, Q.-S., Gong, X.-H., He, Y.-S., 2016. Iron and magnesium isotopic constraints on the origin of chemical heterogeneity in podiform chromitite from the Luobusa ophiolite, Tibet. Geochem. Geophys. Geosyst. 17, 940–953.
Xiao, Y., Teng, F.Z., Zhang, H.F., Yang, W., 2013. Large magnesium isotope fractionation in peridotite xenoliths from eastern North China craton: product of melt-rock interaction. Geochim. Cosmochim. Acta 115, 241–261.
Xu, Y.G., He, B., Chung, S.L., Menzies, M.A., Frey, F.A., 2004. Geologic, geochemical, and geophysical consequences of plume involvement in the Emeishan flood-basalt province. Geology 32, 917–920.
Yang, W., Teng, F.-Z., Zhang, H.-F., 2009. Chondritic magnesium isotopic composition of the terrestrial mantle: a case study of peridotite xenoliths from the North China craton. Earth Planet. Sci. Lett. 288, 475–482.
Zhang, X.-Q., Song, X.-Y., Chen, L.-M., Xie, W., Yu, S.-Y., Zheng, W.-Q., Deng, Y.-F., Zhang, J.-F., Gui, S.-G., 2012. Fractional crystallization and the formation of thick Fe–Ti–V oxide layers in the Baima layered intrusion, SW China. Ore Geol. Rev. 49, 96–108.
Zhang, X.Q., Song, X.Y., Chen, L.M., Yu, S.Y., Xie, W., Deng, Y.F., Zhang, J.F., Gui, S.G., 2013. Chalcophile element geochemistry of the Baima layered intrusion, Emeishan large igneous province, SW China: implications for sulfur saturation history and genetic relationship with high-Ti basalts. Contrib. Mineral. Petrol. 166, 193–209.
Zhang, Z.C., Mahoney, J.J., Mao, J.W., Wang, F.H., 2006. Geochemistry of picritic and associated basalt flows of the western Emeishan flood basalt province, China. J. Petrol. 47, 1997–2019.
Zhong, H., Zhu, W.-G., 2006. Geochronology of layered mafic intrusions from the Pan–Xi area in the Emeishan large igneous province, SW China. Miner. Depos. 41, 599–606.
Zhong, H., Zhu, W.G., Hu, R.Z., Xie, L.W., He, D.F., Liu, F., Chu, Z.Y., 2009. Zircon U–Pb age and Sr–Nd–Hf isotope geochemistry of the Panzhihua A-type syenitic intrusion in the Emeishan large igneous province, southwest China and implications for growth of juvenile crust. Lithos 110, 109–128.

Zhou, M.F., Arndt, N.T., Malpas, J., Wang, C.Y., Kennedy, A.K., 2008. Two magma series and associated ore deposit types in the Permian Emeishan large igneous province, SW China. Lithos 103, 352–368.
Zhou, M.F., Malpas, J., Song, X.Y., Robinson, P.T., Sun, M., Kennedy, A.K., Lesher, C.M., Keays, R.R., 2002. A temporal link between the Emeishan large igneous province (SW China) and the end-Guadalupian mass extinction. Earth Planet. Sci. Lett. 196, 113–122.
Zhu, D., Bao, H., Liu, Y., 2015. Non-traditional stable isotope behaviors in immiscible silica-melts in a mafic magma chamber. Sci. Rep. 5, 17561.